

## Intersubband optical bistability induced by resonant tunneling in an asymmetric double quantum well

Mark I. Stockman,\* Lakshmi N. Pandey, Leonid S. Muratov,\* and Thomas F. George  
*Departments of Physics and Chemistry, Washington State University, Pullman, Washington 99164-2814*  
 (Received 25 January 1993; revised manuscript received 13 May 1993)

An intrinsic optical bistability in a double quantum well is described theoretically. The effect is based on the resonant tunneling of electrons against the electric-field force (the counterfield electron transfer) and is driven and controlled by far-ir radiation exciting an intersubband transition. The theory relies on the density-matrix technique and takes into account optical intersubband excitation, interwell tunneling, the relaxation of populations and polarizations, and the mean-field effects of the transferred electron charge (shifts of the levels and changes of matrix elements). Hysteresis-type curves are obtained for both the charge-transfer probability and the optical absorption as functions of the light intensity. The theory shows the effect to be readily observable under realistic conditions, with the exciting-light intensity as low as  $50 \text{ W/cm}^2$ .

### I. INTRODUCTION

In this paper, we theoretically consider a type of intrinsic optical bistability in semiconductor heterostructures, based on resonant tunneling between the coupled wells in an asymmetric double quantum well. The optical bistability in quantum-well systems has attracted a great deal of attention since the demonstration of self-electro-optic effect devices.<sup>1</sup> Most known types of bistability effects in semiconductor heterostructures are electrical or optoelectrical, i.e., they require consumption of electrical energy from an external source and are accompanied by a dc current in an external circuit (e.g., Refs. 1–7).

Unlike Refs. 1–7, but similar to two recently suggested optical-bistability effects in asymmetric quantum wells,<sup>8,9</sup> an effect considered in this paper is a pure optical bistability, i.e., there is no involvement of a dc current or external electrical-energy dissipation, and no optical cavity is required. Intersubband electronic transitions [also called quantum-well envelope-state transitions (QWEST) (Ref. 10)] drive the effect, and the effect reported in Refs. 8 and 9 are excited and can be monitored by far-ir radiation.

However, our effect is based on resonant tunneling through the barrier separating the two individual wells in a double-well structure, which strongly depends on the

quantum-level alignment. Distinct from this, the mechanisms of neither Ref. 8 nor Ref. 9 incorporate the resonant tunneling. In fact, the electron transfer occurs in Ref. 9 via a level lying above the top of the barrier, with no resonant effects associated with such a transfer. In Ref. 8, the transfer occurs via a dipole transition across the barrier. Such transitions, even though not exactly forbidden, are weak because of the small overlap of the wave functions in the two wells.

The above differences are the principal differences because in our case the resonant dependence of the tunneling rate on the relative positions of the upper levels in the two wells is the major source of the positive feedback, necessary to obtain the bistability. Figure 1, which will be discussed in detail in Sec. II, is an illustration of the changes in the alignment of the upper levels in the two wells in the process of the bistable switching. Another important contribution to the positive feedback in our effect, also caused by the resonant tunneling, is due to the formation of the split-doublet levels that changes the optical-absorption contour (see Sec. II).

As a result of the differences in the mechanism, the intensity (power density) of the radiation required for the bistable switching in our case is estimated to be on the order or less than  $50 \text{ W/cm}^2$ . This is many orders of magnitude less than the intensity of  $4 \text{ MW/cm}^2$  required in

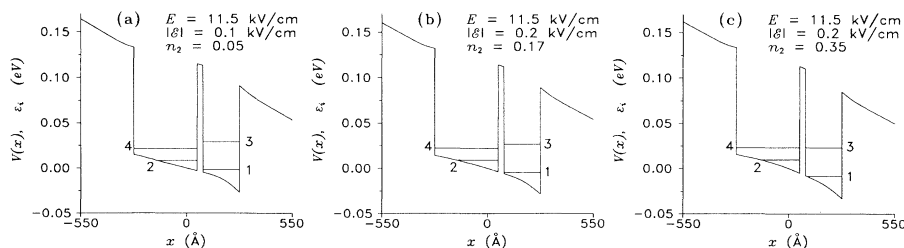


FIG. 1. Potential profile  $V(x)$  of the double well (conduction-band offset) and the energies  $\epsilon_i$  ( $i=1-4$ ) of the lowest levels in the individual wells at low radiation intensity (a) and for a critical intensity of the exciting radiation before the bistable switching (b) and after the switching (c). The wide ( $\mathcal{W}$ ) well is the left and the narrow ( $\mathcal{N}$ ) well is the right one in the double-well structure. The coordinate perpendicular to the well structure is  $x$  (other notations are in the text).

Ref. 8 in the double-well and 80 kW/cm<sup>2</sup> in the triple-well geometry and the intensities of 200–800 kW/cm<sup>2</sup> expected in Ref. 9. Thus, not only the mechanisms but also the properties of our type of the bistability and of the effects of Ref. 8 and 9 differ principally.

Because both the resonant tunneling and nonlinear optical excitation are known to be sensitive to the polarization relaxation (dephasing), we have chosen the density-matrix approach that allows one fully to incorporate dephasing described by nondiagonal elements of the density matrix. In contrast, the rate equations employed in Refs. 8 and 9 do not adequately take into account the dephasing and polarization-saturation effects. One may expect such effects to be important, especially for high light intensities.

To provide the conditions for the present type of the bistability, one should necessarily employ the four-level scheme of the levels in the presence of a constant bias shown in Fig. 1 (see Sec. II). This scheme has been previously considered in our papers,<sup>11,12</sup> where the counterfield electron-transfer (CET) effect has been predicted. The CET is an important process in the mechanism of the present bistability. Distinct from this, Ref. 8 relies on two- and three-level schemes, and Ref. 9 on a three-level scheme.

In Sec. II we introduce and qualitatively describe the present bistability, and in Sec. III we present a quantitative theory. The obtained numerical results are presented in Sec. IV, and the discussion is contained in Sec. V.

## II. QUALITATIVE DESCRIPTION OF EFFECT

To introduce the proposed effect, let us consider an asymmetric quantum well where the electron population of the conduction band is created either by modulation doping or by incoherent near-ir radiation causing interband excitation. We will take into account the space charge of electrons and the electric field associated with it. This field is changed by light-induced transfer of electrons that, in turn, effects this transfer providing a positive feedback necessary for bistability to occur. The electric field found self-consistently takes into account the average Coulomb interaction between the electrons (but, of course, not correlations between them). No other interaction will be considered.

Examples of self-consistent potentials and the two lowest-lying energy levels (which are, of course, offsets of the conduction subbands) in each of the individual wells are shown in Fig. 1. The corresponding states in the narrow ( $\mathcal{N}$ ) well are denoted as  $|1\rangle$  and  $|3\rangle$  and in the wide ( $\mathcal{W}$ ) well as  $|2\rangle$  and  $|4\rangle$ . We note that Fig. 1 actually represents a realistic quantum-well system that will be described below along with the method of computation. The double well is externally electrically biased to make the ground state  $|1\rangle$  in the  $\mathcal{N}$  well the overall ground state of the system and the levels  $|2\rangle$  and  $|4\rangle$  to lie within the pair of levels  $|1\rangle$  and  $|3\rangle$ . Such a sequence of levels shown in Fig. 1(a) is achievable for an asymmetric double quantum well and is necessary for the proposed bistability. An optical (far-ir) radiation driving the effect is assumed to have frequency  $\omega$  close to but somewhat less

(within the linewidth) than the frequency<sup>13</sup>  $\epsilon_{31}$  of the transition between the levels in the  $\mathcal{N}$  well. The excited levels  $|3\rangle$  in the  $\mathcal{N}$  well and  $|4\rangle$  in the  $\mathcal{W}$  well are assumed to be detuned as shown in Fig. 1(a), but not too much, so that there can exist some probability of the electron tunneling  $|3\rangle \leftrightarrow |4\rangle$ .

The origin of the bistability can be described as the following. We start with low-intensity radiation [see Fig. 1(a)]. While optically excited to the  $|3\rangle$  state, electrons tunnel to the  $|4\rangle$  state and then undergo a relaxation transition and accumulate in the  $|2\rangle$  state in the  $\mathcal{W}$  well. This state is comparatively long-lived due to the probability of tunneling between the ground levels  $|2\rangle \leftrightarrow |1\rangle$  being small enough. This is the case because the  $|1\rangle$  and  $|2\rangle$  levels are misaligned, and also the tunneling amplitude for lower-lying states is small. As a net result of these excitation/tunneling/relaxation processes, electrons are transferred from the  $\mathcal{N}$  to  $\mathcal{W}$  well, i.e., against the force exerted by the bias field. This is the essence of the counterfield electron transfer (CET) effect, which we have suggested in Refs. 11 and 12. We note that a change of the bias field produced by the transferred charges and consequent changes of the level energies  $\epsilon_i$  ( $i = 1-4$ ) have not been taken into account in Refs. 11 and 12. As we see below, these changes may result in a strong positive feedback bringing about bistability. Mathematically, such a feedback results in a nonlinear system of master equations, instead of a linear system as in Refs. 11 and 12 (see below).

With an increase of the radiation intensity, the electronic charge accumulated in the  $\mathcal{W}$  well causes an increase of the bias field inside the double well, which reduces the detuning  $\epsilon_{43}$  of the excited states  $|3\rangle$  and  $|4\rangle$ , as shown in Fig. 1(b). This brings about two factors which both further enhance the electron transfer and the bias field, thus providing the necessary positive feedback. The first is a higher rate of tunneling due to the smaller detuning  $\epsilon_{43}$ . The second factor is mixing of the states  $|3\rangle$  and  $|4\rangle$  and formation of split-doublet levels  $|\pm\rangle$ . The exciting radiation becomes more resonant with the lowest level  $|-\rangle$  of this doublet, which also increases the excitation rate.

At this point, the positive feedback described above brings about a rapid increase of the electron-transfer probability (i.e., population  $n_2$  of the  $|2\rangle$  level), the current state of the system [Fig. 1(b)] becomes unstable, and it hops to a state with higher  $n_2$  which is illustrated by Fig. 1(c). In this state, the level  $|4\rangle$  is already slightly higher than  $|3\rangle$ . Therefore, any additional electron transfer would result in an increased detuning  $|\epsilon_{34}|$ . This brings about stabilization of the system. Now, the intensity of the radiation may be decreased, but efficient resonant excitation and transfer will sustain the resonant state of the system shown in Fig. 1(c), which means hysteresis as usual for bistability.

To avoid any confusion, we note that the energy levels presented in Fig. 1 belong to electronic states found for two uncoupled wells. These states form a basis in which we consider the interwell tunneling and different relaxation processes. As already mentioned above, tunneling brings about the mixing of states of the individual wells

and formation of the split-doublet levels. The polarization relaxation, on the other hand, suppresses the coherent tunneling and its manifestations. These effects along with radiation excitation are taken into account within the density-matrix technique.

### III. QUANTITATIVE THEORY

Elementary processes to be taken into account comprise radiative excitation in both of the wells, the electron tunneling between the wells, and the relaxation of populations and polarizations. As emphasized above in Sec. II, the electric field induced by the electron charges and its influence on one-electron states, tunneling amplitude, and the optical excitation rate are of principal importance and will also be included.

We shall consider the problem quantitatively employing the density-matrix technique in the basis of the four states  $|i\rangle$  ( $i=1-4$ ) in the individual wells. We note that distances in energy to the next states in the wells are large (approximately proportional to the quantum number), which justifies this truncated scheme of levels. Because subbands are parallel and photon momentum is negligibly small, electron momentum (which is parallel to the heterostructure plane) vanishes from the equation of motion for the density matrix  $\rho$ . This equation has the familiar form<sup>13</sup>

$$\dot{\rho} = i[\rho, H] - R, \quad (1)$$

where  $\dot{\rho} \equiv \partial\rho/\partial t$ ,  $H$  is the Hamiltonian,  $[, ]$  denotes a commutator, and  $R$  is a relaxation matrix (collision integral). For  $R$  we adopt the model of relaxation constants similar to Ref. 12. The Hamiltonian is the sum of the energy in the well, interaction with the electromagnetic field, and a tunneling part,  $H = H_0 + H_{em} + H_t$ , where  $(H_0)_{ij} = \varepsilon_i \delta_{ij}$ . Considering an exciting optical wave with (electrical) amplitude  $\mathcal{E}$  and frequency  $\omega$ , we have  $(H_{em})_{ij} = -\mathbf{d}_{ij}[\mathcal{E}e^{-i\omega t} + \text{c.c.}]$ , where  $\mathbf{d}_{ij}$  are dipole matrix elements and  $i, j = 1, 3$  or  $i, j = 2, 4$ . As discussed above (see also Ref. 12), tunneling between only the excited states is taken into account, which implies that  $(H_t)_{43} = (H_t)_{34}^* = \tau$ , where  $\tau = \text{const}$  is a tunneling amplitude.

For simplicity, we shall consider the temperature  $T$  to be sufficiently low,  $T \ll \varepsilon_{21}, \tau$ , so that  $T$  vanishes from the equations. Realistically, assuming that  $\mathcal{E}$  is not too large, which implies that field broadening of the levels is much less than the transition frequencies, i.e.,  $|\mathcal{E}\mathbf{d}| \ll \varepsilon_{ij}$ , we can use the rotating-wave approximation (RWA), also known as the resonant approximation. In the RWA, the temporal dependencies of the population numbers  $n_i = \rho_{ii}$  and nondiagonal matrix elements have the forms  $\rho_{13} = \rho_{31}^* = \bar{\rho}_{13}e^{i\omega t}$ ,  $\rho_{14} = \rho_{41}^* = \bar{\rho}_{14}e^{i\omega t}$ ,  $\rho_{23} = \rho_{32}^* = \bar{\rho}_{23}e^{i\omega t}$ ,  $\rho_{24} = \rho_{42}^* = \bar{\rho}_{24}e^{i\omega t}$ ,  $\rho_{12} = \rho_{21}^* = \bar{\rho}_{12}$ , and  $\rho_{34} = \rho_{43}^* = \bar{\rho}_{34}$ , where  $\bar{\rho}_{ij}$  are slowly varying amplitudes. Substituting these expressions into Eq. (1) and retaining only resonantly enhanced terms, we obtain a system of equations in the RWA, containing no terms oscillating with the optical frequency  $\omega$ ,

$$\begin{aligned} \dot{n}_1 &= 2 \text{Im}(\bar{\rho}_{13}G_{31}) + \gamma_2 n_2 + \gamma_3 n_3, \\ \dot{n}_2 &= 2 \text{Im}(\bar{\rho}_{24}G_{42}) - \gamma_2 n_2 + \gamma_4 n_4, \\ \dot{n}_3 &= -2 \text{Im}(\bar{\rho}_{13}G_{31} + \bar{\rho}_{34}\tau) - \gamma_3 n_3, \\ \dot{n}_4 &= -2 \text{Im}(\bar{\rho}_{24}G_{42} - \bar{\rho}_{34}\tau) - \gamma_4 n_4, \\ \dot{\bar{\rho}}_{12} + (-i\varepsilon_{21} + \Gamma_{12})\bar{\rho}_{12} &= -i\bar{\rho}_{14}G_{42} + iG_{31}^*\bar{\rho}_{23}^*, \\ \dot{\bar{\rho}}_{13} + [i(\omega - \varepsilon_{31}) + \Gamma_{13}]\bar{\rho}_{13} &= -in_{13}G_{31}^* + i\bar{\rho}_{14}\tau, \\ \dot{\bar{\rho}}_{14} + [i(\omega - \varepsilon_{41}) + \Gamma_{14}]\bar{\rho}_{14} &= i\bar{\rho}_{13}\tau^* + iG_{31}^*\bar{\rho}_{34} - i\bar{\rho}_{12}G_{42}^*, \\ \dot{\bar{\rho}}_{23} + [i(\omega - \varepsilon_{32}) + \Gamma_{23}]\bar{\rho}_{23} &= i\bar{\rho}_{24}\tau + iG_{42}^*\bar{\rho}_{34}^* - i\bar{\rho}_{12}G_{31}^*, \\ \dot{\bar{\rho}}_{24} + [i(\omega - \varepsilon_{42}) + \Gamma_{24}]\bar{\rho}_{24} &= -in_{24}G_{42}^* + i\bar{\rho}_{23}\tau^*, \\ \dot{\bar{\rho}}_{34} + (-i\varepsilon_{34} + \Gamma_{34})\bar{\rho}_{34} &= in_{34}\tau^* + iG_{31}\bar{\rho}_{14} - i\bar{\rho}_{23}^*G_{42}^*. \end{aligned} \quad (2)$$

Here,  $n_{ij} = n_i - n_j$ ,  $\varepsilon_{ij} = \varepsilon_i - \varepsilon_j$ ,  $\gamma_i$  is a decay constant of the  $|i\rangle$  state,  $\Gamma_{ij}$  is a polarization-relaxation constant for the transition  $|i\rangle \leftrightarrow |j\rangle$ ,  $\Gamma_{ij} = \frac{1}{2}(\gamma_i + \gamma_j) + \bar{\Gamma}_{ij}$ , where  $\bar{\Gamma}_{ij}$  is the corresponding pure-depolarization constant, and  $G_{ij} = \mathcal{E}\mathbf{d}_{ij}$  is the Rabi frequency for the corresponding transition.

Equations (2) are complemented with self-consistency equations,

$$-\frac{1}{2} \frac{d}{dx} \frac{1}{m^*} \frac{d}{dx} \Psi_i + V(x)\Psi_i = \varepsilon_i \Psi_i, \quad (3)$$

$$V(x) = U(x) - eE(x - x_1)$$

$$-\frac{4\pi}{\epsilon} e \int_{x_1}^x dx' \int_{x_0}^{x'} v(x'') dx'', \quad (4)$$

$$v(x) = eN \sum_{i=1}^4 n_i |\Psi_i(x)|^2 - e\nu_{ci}(x). \quad (5)$$

Here, the Schrödinger equation (3), where  $m^*$  is the effective electron mass, is to be solved for two uncoupled wells ( $\mathcal{N}$  and  $\mathcal{W}$ ) to obtain the one-electron wave functions  $\Psi_i$ , energies of the levels  $\varepsilon_i$ , and dipole moments  $\mathbf{d}_{31}$  and  $\mathbf{d}_{42}$ . The potential profile of the structure  $V(x)$  is given by Eq. (4), where  $U(x)$  is the conduction-band offset in the heterostructure forming two quantum wells. The last two terms in Eq. (4) yield the electrostatic potential obtained as a solution of the one-dimensional Laplace equation, where  $e$  is the electron charge,  $\epsilon$  is an average dielectric constant of the heterostructure material,  $\nu(x)$  is the space-charge density of electrons and counterions,  $E$  is the external bias field,  $x_0$  is any point positioned outside the charge-containing region, and  $x_1$  is an arbitrary point where the electric potential is set as zero (in the calculations,  $x_0$  is positioned at the left edge of the well structure and  $x_1$  in its center). The density  $\nu(x)$  is determined by Eq. (5), where  $\nu_{ci}$  is a density of counterions (ionized dopants) which we assume to be distributed in the barrier regions (modulation doping), and  $N$  is the average two-dimensional density of conduction-band electrons, with the electrical neutrality condition implied,  $N = \int \nu_{ci}(x) dx$ .

Mathematically, Eqs. (2)–(5) form a nonlinear system

of equations. Examination of Eqs. (3)–(5) shows that feedback described by these equations is characterized by a dimensionless coupling constant  $g = e^2 m^* L_0^3 N / \hbar^2 \epsilon$  (here we indicate  $\hbar$ ), where  $L_0$  is the total thickness of the coupled wells, and the feedback is strong for  $g \gg 1$ .

We have solved Eqs. (2)–(5) numerically for the stationary case ( $\dot{n}_i = 0$  and  $\dot{\rho}_{ij} = 0$ ). Because any numerical procedure of finding the solution for a given optical field  $\mathcal{E}$  becomes unstable for  $\mathcal{E}$  approaching the region of the bistability, we have alternatively chosen  $n_2$ , which is the probability of transfer of electrons into the  $\mathcal{W}$  well, to be an independent variable. This yields a stable numerical procedure since the solution is a single-valued function of  $n_2$ .

A solution of Eqs. (2)–(5) has been found by means of an iterative procedure (see below), changing  $n_2$  by small steps. For each  $n_2$  we use the solution of the previous step as an initial set. Doing so, from Eq. (2) using the Newton-Raphson method we find  $\mathcal{E}$  and also  $n_1$ ,  $n_3$ ,  $n_4$ , and  $\bar{\rho}_{ij}$ . Substituting those into Eqs. (5) and (4), we find  $V(x)$ . With this and using the sixth-order Runge-Kutta method and the shooting algorithm, we solve Eq. (3) to obtain new  $\Psi_i$  and  $\epsilon_i$ . Finally, calculating new  $G_{31}$  and  $G_{42}$  we complete the iteration. Not more than three such iterations have been needed to converge.

#### IV. NUMERICAL RESULTS

Below we present results as obtained from the numerical procedure (see above). One series of the results is concerned with the dependence between the electron transfer probability  $n_2$  and the optical field amplitude  $\mathcal{E}$ . Note that experimentally  $n_2$  can be monitored electrically as discussed below in Sec. V. Another observable quantity whose behavior is examined below is the optical absorption  $P$ , which we calculate as the absorption rate (photons of the exciting radiation per unit time) per one electron per double well,

$$P = \frac{1}{\omega} \left\langle \mathcal{E}(t) \frac{d}{dt} \text{Tr}(\mathbf{d}\rho(t)) \right\rangle = \gamma_3 n_3 + \gamma_4 n_4. \quad (6)$$

Here, the first equality is a definition, and the second represents the final result obtained using Eq. (2).

As a realistic example, we consider GaAs quantum wells (330 and 190 Å) formed by  $\text{Al}_{0.15}\text{Ga}_{0.85}\text{As}$  barriers (900, 30, and 900 Å). The dependence of the band offsets  $U(x)$  and effective mass  $m^*$  on the chemical composition of the wells is adopted from Ref. 14. Counterions are placed adjacent to the wells in the external barriers, uniformly distributed in 100-Å layers. The total concentration of electrons (equal to this of counterions) is considered to be in the range  $N = 2 \times 10^{10} - 10^{11} \text{ cm}^{-2}$ . For such concentrations, the system under consideration is characterized by the range of the coupling parameter  $g = 3 - 15$  and, consequently, belongs to the cases of moderate to strong positive feedback. We note that Fig. 1 is a numerically accurate illustration of the described double-well system and the solutions (for  $N = 10^{11} \text{ cm}^{-2}$ ). We point out that the interlevel separation  $\epsilon_{21}$  is greater than 11 meV, while the Fermi energy for electrons in the  $|1\rangle$  subband is less than 3.5 meV. Thus, only the  $\mathcal{N}$  well

is initially populated, as assumed in the theory.

We set for the optical frequency  $\omega = 30 \text{ meV}$ , so that  $\omega$  is somewhat less than the optical transition frequency,  $\epsilon_{31} = 31 \text{ meV}$ , which is favorable for the bistability effect, as discussed above in Sec. II. We emphasize that  $\omega$  is less than the (longitudinal) optical-phonon frequency  $\omega_0 \approx 36 \text{ meV}$ . Thus, emission of optical phonons is suppressed, which dramatically diminishes the polarization relaxation and brings about narrower spectral contours of intersubband absorption, as studied in Ref. 15. This allows us to choose realistically the decay, dephasing, and tunneling constants similarly to Ref. 12 as  $\gamma_3 = \gamma_4 = 0.1 \text{ meV}$ ,  $\bar{\Gamma}_{12} = \bar{\Gamma}_{13} = \bar{\Gamma}_{14} = \bar{\Gamma}_{23} = \bar{\Gamma}_{24} = 1 \text{ meV}$ ,  $\bar{\Gamma}_{34} = 1.4 \text{ meV}$ , and to calculate  $\tau = 2.5 \text{ meV}$ .

The data for the case of the highest electron density considered,  $N = 10^{11} \text{ cm}^{-2}$ , which corresponds to strong coupling, are presented in Fig. 2 for three values of the bias field  $E$ . We can see a pronounced bistability and hysteresis for all three values of  $E$ . For  $E = 11.5 \text{ kV/cm}$  we indicate by arrows the contour of the hysteresis and by asterisks the points of bistable switching, where both  $n_2$  and  $P$  are changed several-fold. The point of a bistable switching upward [for  $E = 11.5 \text{ kV/cm}$ , labeled by  $b$  in Fig. 2(a)] quantitatively corresponds to Fig. 1(b), where the  $|4\rangle$  level is already close but still somewhat lower than  $|3\rangle$ . The bistable switching brings the system to the

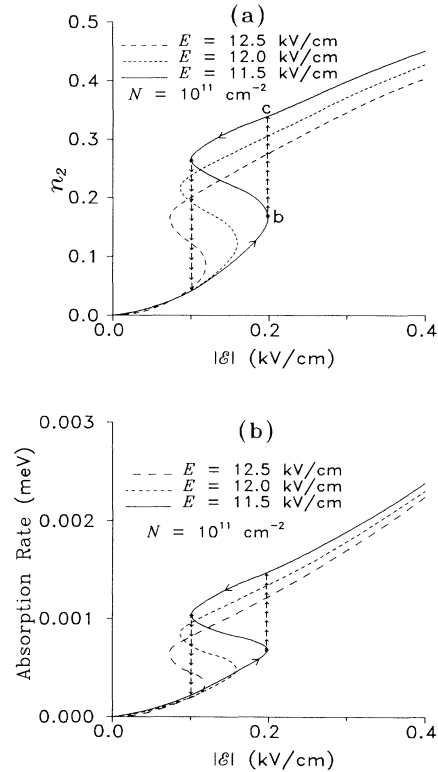


FIG. 2. Bistability in the double quantum well: transfer probability  $n_2$  (a) and absorption rate  $P$  (b) plotted against the exciting wave amplitude  $\mathcal{E}$  for different bias fields  $E$  and for an electron concentration of  $N = 10^{11} \text{ cm}^{-2}$ , as indicated. The asterisks indicate points of bistable switching and the vertical arrows their directions.

point  $c$  [Fig. 2(a)], which corresponds to Fig. 1(c), where we can see some “overshooting”: the level  $|4\rangle$  becomes slightly higher than  $|3\rangle$ . This implies that the positive feedback changes to negative and the system is stabilized. As usual, the states of the system corresponding to the backward-bending portion of the curve [between the asterisks in Fig. 1(a)] are unstable, as confirmed numerically. With a change of  $E$  within 1 kV/cm, the curves in Fig. 2(a) shift and somewhat change in the amplitude, but are not principally modified. The bistability occurs at the optical field amplitude  $\mathcal{E} \approx 0.1$  kV/cm corresponding to a light intensity of  $50 \text{ W/cm}^2$ , which is comparatively low and easily achievable.

The optical absorption [Fig. 2(b)] behaves very similar to the transfer probability [Fig. 2(a)]. In particular, with an increase of light intensity in the transition region, absorption is *increased*. In some known systems, intensifying the optical excitation depopulates the initial state and *decreases* the absorption (as is the case in, e.g., Ref. 1). However, in Ref. 9 the absorption increases, and this increase is the single source of the positive feedback. In the proposed bistable system, such a behavior is due to quantum delocalization of the states over both the wells brought about by the resonant tunneling. Specifically, in the transition region, the lower component  $|-\rangle$  of the split-level doublet formed by  $|3\rangle$  and  $|4\rangle$  becomes resonant with the exciting radiation and acquires a considerable oscillator strength causing an additional absorption.

With the electron concentration  $N$  down to  $5 \times 10^5 \text{ cm}^{-2}$  (corresponding to  $g \approx 7$ ), as illustrated by Fig. 3,

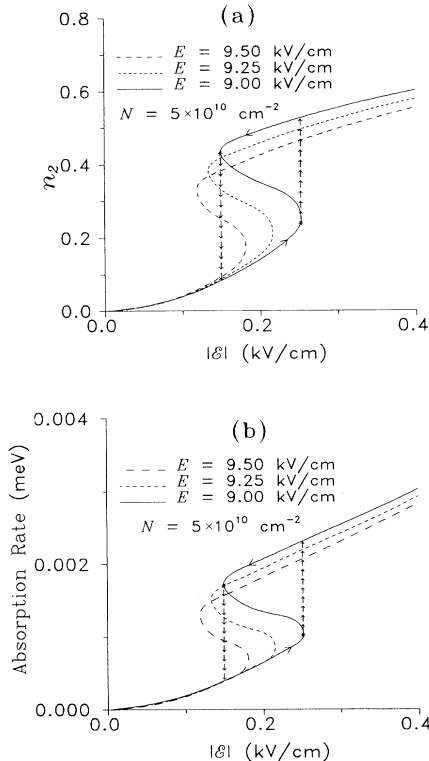


FIG. 3. The same as in Fig. 2, but for  $N = 5 \times 10^{10} \text{ cm}^{-2}$ .

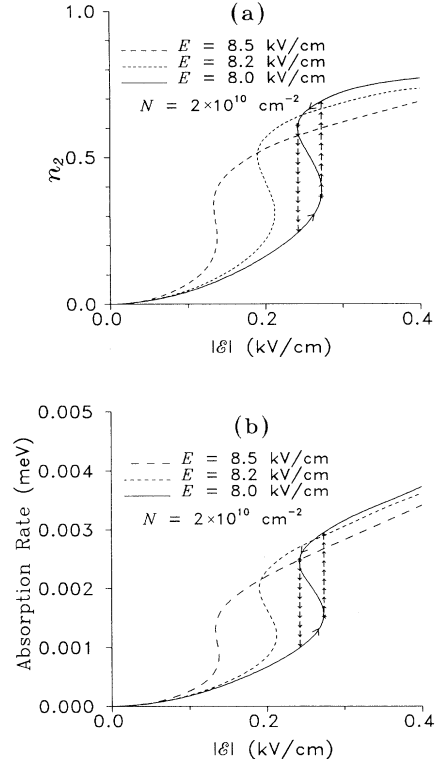


FIG. 4. The same as in Fig. 2, but for  $N = 2 \times 10^{10} \text{ cm}^{-2}$ .

the region of bistability is shifted toward larger biases, as expected (the field created by the electrons acts in the same direction as the bias field). At the same time, neither the shapes nor amplitudes of the hysteresis loops are changed. We note that relative to the field  $\mathcal{E}$ , the bistability is less pronounced, as we can expect for smaller  $g$ .

A qualitative change occurs at  $N = 2 \times 10^{10} \text{ cm}^{-2}$  ( $g \approx 3$ ), as seen in Fig. 4. In this case, the bistability exists in only a rather narrow range of  $\mathcal{E}$ . We note that in all three cases presented above (Figs. 2–4), the shapes of the dependences of both  $n_2$  and  $P$  in the region of bistability are very similar. Upon further decrease of the electron concentration to the critical one,  $N^* \approx 1.8 \times 10^{10} \text{ cm}^{-2}$ , the hysteresis loop completely degenerates to a line and the bistability disappears. Thus, the described bistability effect is of the threshold nature and exists only in a certain range of parameters. This is simply a matter of fact that this parameter range is realistic for the GaAs/Al<sub>x</sub>Ga<sub>1-x</sub>As system considered with the light intensity as low as  $\lesssim 50 \text{ W/cm}^2$ .

## V. DISCUSSION

Above in Secs. III and IV, we have presented a theory of nonlinear optical excitation in a double quantum well with account taken of the effects of the electric field generated by spatial charge of electrons. This field, changing the positions of quantum levels and, consequently, the rates of the resonant tunneling and optical excitation, brings about a strong positive feedback resulting in an

optical bistability. This bistability occurs at the intensities of the exciting radiation in the range below  $100 \text{ W/cm}^2$ , which is three to four orders of magnitude lower than in the two other proposed intersubband bistabilities.<sup>8,9</sup> This makes the present effect promising for applications.

The present bistability is a threshold effect and exists only in a certain region of parameters. The actual parameters of GaAs/Al<sub>x</sub>Ga<sub>1-x</sub>As heterostructures allow the effect to exist. For the double quantum well considered above, the bistability is predicted for an electron concentration  $N$  higher than the threshold value  $N^* \approx 1.8 \times 10^{10} \text{ cm}^{-2}$ . For the values of  $N \sim 10^{11} \text{ cm}^{-2}$ , for which the employed model of the electron gas in a self-consistent electric potential is a reasonable approximation, the bistability is strongly pronounced, accompanied by severalfold changes of electron charges and absorption. Instead of further discussing the effect, we will concentrate below on its expected experimental manifestations and some prospective applications.

The considered bistability manifests itself in sudden changes of the intersubband absorption at the switching points, as illustrated by Figs. 2(b), 3(b), and 4(b), and can be observed on the basis of these changes. Also, as follows from these figures, in a vicinity of the bistability, a double quantum well is a strongly nonlinear optical absorber. As discussed above, an unusual feature of this bistability is that with the switching induced by an increasing light intensity, the absorption also increases. This implies that the absorption nonlinearity is positive. One of the possible applications of this effect may be stabiliza-

tion of the intensity of far-ir radiation, including lasers. We note that such a system at the threshold of the bistability possesses certain advantages for this application.

A sudden transfer of electrons between two coupled wells at the points of transitions between the two stable states brings about also a *transient* current (pulse) in an external circuit due to capacitive coupling. The total charge  $Q$  transferred externally per switching is given by

$$Q = eSN\Delta n_2\Delta x / L, \quad (7)$$

where

$$\Delta x = \int_{-\infty}^{\infty} [|\Psi_1(x)|^2 - |\Psi_2(x)|^2]x dx,$$

$\Delta x$  has the meaning of an effective distance over which the charge is transferred,  $\Delta n_2$  is the change of  $n_2$  resulted from switching,  $L$  is the size of the quantum-well structure (conductive regions are supposed to surround this structure, Ohmically coupled to external leads), and  $S$  is the illuminated area. For the example of Fig. 1,  $L = 1100 \text{ \AA}$ , and we have calculated  $\Delta x = -77 \text{ \AA}$ . Thus,  $|\Delta x|/L = 0.07$ , which means that  $Q$  may realistically constitute  $\approx 7\%$  of the internally transferred charge and is readily measurable.

#### ACKNOWLEDGMENTS

This research was supported by the National Science Foundation under Grant No. CHE-9196214 and by the Pittsburgh Supercomputing Center under grant No. PHY890020P.

\*Also with Institute of Automation and Electrometry, Russian Academy of Sciences, 630090 Novosibirsk, Russia.

<sup>1</sup>D. A. B. Miller, D. S. Chemla, T. C. Damen, A. C. Gossard, A. Wiegmann, T. H. Hood, and C. A. Burrus, Appl. Phys. Lett. **45**, 13 (1984).

<sup>2</sup>A. Zrenner, J. M. Worlock, L. T. Florez, and J. P. Harbison, Appl. Phys. Lett. **56**, 1763 (1990).

<sup>3</sup>P. England, J. E. Golub, L. T. Florez, and J. P. Harbison, Appl. Phys. Lett. **58**, 887 (1991).

<sup>4</sup>K. L. Jensen and F. A. Buot, Phys. Rev. Lett. **66**, 1078 (1991).

<sup>5</sup>R. Döttling and E. Schöll, Phys. Rev. B **45**, 1935 (1992).

<sup>6</sup>J. Zang and J. Birman, Phys. Rev. B **46**, 5020 (1992).

<sup>7</sup>W. I. E. Tagg, M. S. Skolnick, M. T. Emeny, A. W. Higgs, and C. R. Whitehouse, Phys. Rev. B **46**, 1505 (1992).

<sup>8</sup>J. Khurgin, Appl. Phys. Lett. **54**, 2589 (1989).

<sup>9</sup>M. Seto and M. Helm, Appl. Phys. Lett. **60**, 859 (1992).

<sup>10</sup>L. C. West and S. J. Eglash, Appl. Phys. Lett. **46**, 1156 (1985).

<sup>11</sup>M. I. Stockman, L. S. Muratov, L. N. Pandey, and T. F. George, Phys. Lett. A **163**, 233 (1992).

<sup>12</sup>M. I. Stockman, L. S. Muratov, L. N. Pandey, and T. F. George, Phys. Rev. B **45**, 8550 (1992).

<sup>13</sup>We use the system of units in which  $\hbar = 1$  and, consequently, make no distinction between frequency and energy and between wave vector and momentum.

<sup>14</sup>L. N. Pandey and T. F. George, J. Appl. Phys. **69**, 2711 (1991).

<sup>15</sup>M. O. Manasreh, F. Szmulovich, D. V. Fischer, K. R. Evans, and C. E. Stutz, Appl. Phys. Lett. **57**, 1790 (1990).